International Journal of Advances in Engineering and Management (IJAEM)
Volume 8, Issue 1 Jan. 2026, pp: 375-390 www.ijaem.net ISSN: 2395-5252

Contribution to robust control for the regulation of a three-machine parallel system in order to ensure power grid stability

BORARA Bevanona Amelien, RABEARIVELO Apotheken Gericha, ANDRIATSIHOARANA Harlin Samuel
[1, 2, 3] *ED-STII, University of Antananarivo, Madagascar*

Date of Submission: 12-01-2026 Date of Acceptance: 28-01-2026

ABSTRACT: This paper presents a cascade control approach applied to voltage and frequency regulation of a multi-machine power network composed of three synchronous generators and six interconnected nodes. The main objective is to improve system stability under disturbances while guaranteeing steady-state robustness.

The proposed control structure consists of two levels. The local level uses a robust H∞ controller, designed for each generator, to ensure individual voltage and frequency regulation despite parametric uncertainties. The global level aims to suppress inter-machine interactions. It is derived from the overall network equation by treating interactions as a compensating control term subtracted from the global dynamic equations.

System performance is evaluated through simulations in MATLAB/Editor. The results highlight robust stability and robust performance in both transient and steady-state regimes. The proposed controllers prove effective under severe disturbance tests, notably a simulated short circuit, confirming that the cascade scheme can maintain voltage and frequency within acceptable limits.

KEYWORDS: Robust H∞ control, cascade control, voltage–frequency regulation, multi-machine system, stability, MATLAB/Editor.

I. INTRODUCTION

Voltage and frequency stability is a major challenge in the control of interconnected power systems. In a multi-machine network, dynamic interactions among generators are one of the main causes of stability problems because they can generate power oscillations and degrade regulation quality.

The paper by Gupta S. et al. (2015) [1] provides a concrete illustration: in a multi-machine power network, each synchronous generator (with its inertia, excitation system, and governor) does not operate in isolation. Power flows between machines through transmission lines mean that changes in one generator affect the others. For example, if generator A injects more power following a fault or a control action, this modifies the voltage at its bus, and therefore modifies the power injection or the power balance of generator B. This feedback constitutes an interaction. Such interactions may lead to electromechanical energy oscillations (wider rotor oscillations, inter-area modes) or even loss of synchronism if they are not properly damped or controlled. Hence, angular/transient stability does not depend only on the local machine but on the overall coupling of the multi-machine network. In practice, stronger coupling can make the system more coherent, but also more vulnerable to low-frequency modes when damping is weak. This is why, in this work, we propose a control system capable of eliminating these interactions.

Given the growing complexity of modern grids—characterized by strong interconnection, the integration of new energy sources of diverse nature, the increased use of power-electronic devices as interfaces or control devices, and the presence of disturbances—it becomes essential to design control laws that ensure stability, performance, and robustness simultaneously.

Several studies have addressed methods for ensuring stability of multi-machine power networks. For instance:

2007: N. Abu-Tabak et al. proposed an approach based on optimal control to improve dynamic stability by increasing the damping of electromechanical oscillations due to inter-machine interactions [2].

2008: N. Abu-Tabak, in his PhD thesis, proposed a stabilization method based on static state-feedback and a Luenberger observer, aiming to improve dynamic stability [3].

2010: Y. Anhong Liu et al. presented a new H∞ excitation control approach for multi-machine, multi-load power systems using the Hamiltonian function method. The objective is to improve dynamic stability by reformulating the power system as a dissipative Hamiltonian system, enabling an energy-based control design [4].

International Journal of Advances in Engineering and Management (IJAEM)
Volume 8, Issue 1 Jan. 2026, pp: 375-390 www.ijaem.net ISSN: 2395-5252

2012: Khodabakhshian et al. applied Quantitative Feedback Theory (QFT) to the decentralized design of power system stabilizers (PSS) for multi-machine systems with parametric uncertainties [5].

2023: Fathollahi et al. introduced a nonlinear fractional-order stabilizer to enhance transient stability, based on synergetic control theory, optimized using an evolutionary algorithm inspired by fish migration behavior to maximize damping of inter-area and local oscillations [6].

2024: Fathollahi et al. also proposed a fractional-order excitation stabilizer based on model-free control, using an ultra-local law capable of estimating unknown dynamics in real time, to avoid dependence on complex uncertain models [7].

This work proposes a cascade control combining: a local robust H∞ regulation, applied individually to each generator, and a global control acting on the interaction among synchronous generators (SG).

The local level stabilizes each machine independently, while the global level is designed to eliminate interactions so that local controllers can operate without being disrupted. The approach is applied to a three-SG, six-node network modeled in MATLAB/Editor. The paper presents system modeling, controller design, and a comparative performance analysis under disturbed conditions.

II. CONTEXT OF STABILITY PROBLEMS IN A MULTI-MACHINE POWER NETWORK

II-1. Stability

Power-system stability is the ability of an electrical energy system, for a given initial operating condition, to regain the same state or another equilibrium state after a disturbance, while keeping most system variables within limits so that the entire system remains in normal operation. Stability is usually divided into three categories: rotor-angle stability (angular stability), voltage stability, and frequency stability [8] [9]. Figure 1 shows the classification used to analyze and address instability problems in power systems.

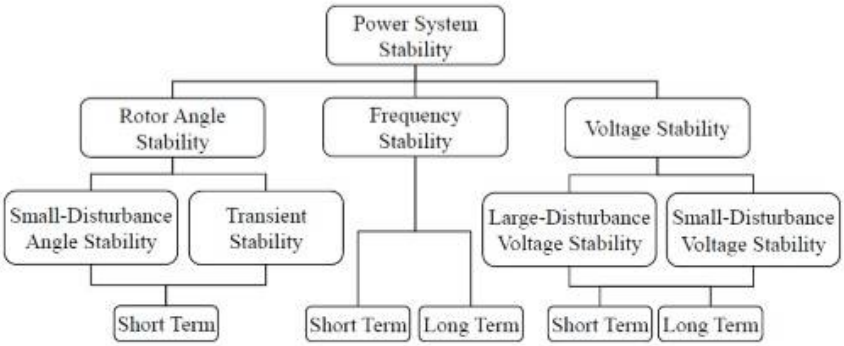

Figure 1: Classification of different types of stability [8] [9].

II-2. Instability

As soon as a network includes several interconnected generators, it becomes dynamically complex, sensitive to disturbances, and exposed to multiple instability mechanisms. The following table summarizes the main causes of instability.

Table 1: Causes of instability in a multi-machine power network [09] [10] [11].

Instability type	Causes
Rotor-angle instability	Loss of synchronism between generators; poorly damped electromechanical oscillations.
Voltage instability	Insufficient reactive power; interaction between machines and loads.
Frequency instability	Imbalance between generation and consumption.

II-3. Effects of Interactions Between Generators

Another cause of instability in a multi-machine power network is inter-generator interaction. Why?

To answer this question, let us consider first the network used by N. Abu-Tabak (2008) in his PhD thesis [3], whose configuration is shown in Figure 2. It is a 50 Hz nominal-frequency network with three synchronous generators $(G_1, G_2$ and $G_3)$ supplying three loads.

International Journal of Advances in Engineering and Management (IJAEM)
Volume 8, Issue 1 Jan. 2026, pp: 375-390 www.ijaem.net ISSN: 2395-5252

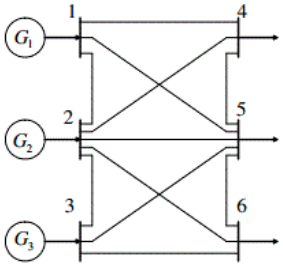

Figure 2: Studied power network

To directly visualize the dynamic effects of inter-machine interactions, we first model this system. In this case, the following data are required [3].

Table 2: Transmission line data

Line	Resistance (pu)	Reactance (pu)
1 – 2	0.10	0.20
1 – 4	0.05	0.20
1 – 5	0.08	0.30
2 – 3	0.05	0.25
2 – 4	0.05	0.10
2 – 5	0.10	0.30
2 – 6	0.07	0.20
3 – 5	0.12	0.26
3 – 6	0.02	0.10
4 – 5	0.20	0.40
4 – 6	0.10	0.30

Table 3: Generator and Excitation System Data

	$M(s)$	$K_D(pu)$	$X_q(pu)$	$X'_d(pu)$	$X_d(pu)$	$T'_{d0}(s)$	$K_A(pu)$	$T_A(pu)$	$K_f(pu)$	$T_f(pu)$	$K_e(pu)$	$T_e(pu)$
G1	9.26	2.5	0.57	0.2	1.02	7.76	50	0.02	0.05	0	1	0
G2	4.61	4	1.66	0.32	1.68	4	50	0.02	0.05	0	1	0
G3	4.61	6	1.66	0.32	1.68	4	50	0.02	0.05	0	1	0

Table 4: System Equilibrium State

Bus Type	$V(pu)$	θ(deg)	$P_{tot}(pu)$	$Q_{tot}(pu)$	$P_g(pu)$	$Q_g(pu)$	$P_l(pu)$	$P_l(pu)$
Ref 1	1.0500	0.0000	0.5484	0.3041	0.5484	0.3041	0.0000	0.0000
PV 2	1.0500	-0.8426	0.9000	0.5852	0.9000	0.5852	0.0000	0.0000
PV 3	1.0500	-1.6080	0.6000	0.5601	0.6000	0.5601	0.0000	0.0000
PQ 4	1.0046	-2.2830	-0.6000	-0.4000	0.0000	0.0000	-0.6000	-0.4000
PQ 5	0.9891	-3.0893	-0.6000	-0.5000	0.0000	0.0000	-0.6000	-0.5000
PQ 6	1.0051	-3.7835	-0.8000	-0.4000	0.0000	0.0000	-0.8000	-0.4000

Where:
K_A, T_A : Gain and time constant of the voltage regulator (pu);
K_e, T_e : Exciter parameters (pu);
K_f, T_f : Stabilizer parameter (pu);
T'_{d0} : Transient time constant of the open circuit (seconds);
K_D : Mechanical damping coefficient (pu);
X'_d: Transient reactance (pu);
X_q : Quadrature-axis stator reactance (pu);
X_d : Direct-axis stator reactance (pu);
$M = 2H$: Mechanical time constant (s);
g: Generated;
l: Consumed;
tot: Total.
V: Voltage magnitude;
θ: Voltage phase angle;
P: Active power;
Q: Reactive power.

Table 5: Current Injected at the Buses

Bus	1	2	3
$\bar{I}$(pu)	0.05223 – 0.2896j	0.8489 – 0.5699j	0.5562 – 0.5493j

Bus	4	5	6
$\bar{I}$(pu)	– 0.5809 – 0.4216j	–0.5785 + 0.5375j	–0.7679 + 0.4496j

The final admittance matrix:

$$\bar{Y}_f = \begin{bmatrix} 0.4080 - j2.3445 & 0.0946 + j1.0147 & 0.0714 + j0.7998 \\ 0.0946 + j1.0147 & 0.2074 - j2.1251 & 0.1243 + j0.6881 \\ 0.0714 + j0.7998 & 0.1243 + j0.6881 & 0.2431 - j1.9249 \end{bmatrix}$$

The voltages behind the transient reactance X'_d:

$$\bar{E} = [1.1079 + j0.1045 \quad 1.2323 + j0.2562 \quad 1.2253 + j0.1485]$$

$$\delta = [5.3883 \quad 11.7447 \quad 6.9102] \quad (\text{deg})$$

Our study will focus on the stability of the voltage and frequency at the output of the interconnected alternators. Consequently, it is important to make the following assumptions [2][3]:

- The three-phase network behavior is balanced, and therefore it is possible to work with the single-phase representation of the network.

For the synchronous machines, the following assumptions are taken into account:

- The machines are salient-pole;
- Saturation is neglected, resulting in self and mutual inductances being independent of

International Journal of Advances in Engineering and Management (IJAEM)
Volume 8, Issue 1 Jan. 2026, pp: 375-390 www.ijaem.net ISSN: 2395-5252

the currents flowing in the various windings;
- The electromotive forces are distributed sinusoidally in the machine air gap, and there is symmetry with respect to the rotor's magnetic axis;
- Slots are assumed to be non-existent;
- Hysteresis and eddy currents in the magnetic parts are not considered;
- The derivative terms $d\psi_d/dt$ and $d\psi_q/dt$ are neglected in the stator model because these terms decay very rapidly;
- The effect of damper windings in the rotor is neglected. This reduces the order of the system under study and minimizes the number of parameters to be known concerning the dampers, which are often unavailable.

II-3-1. Global Nonlinear Model of the Multi-Machine Power Network

The complete model is based on the third-order synchronous machine model, the excitation system model, the interaction model between interconnected machines, and auxiliary equations [3][8].

- Synchronous machine and excitation system model:

$$\frac{d\omega_{ri}}{dt} = -\frac{1}{M_i}\left(T_{mi} - T_{ei} - K_{Di}(\omega_{ri} - 1)\right)$$
$$\frac{d\delta_i}{dt} = \omega_0(\omega_{ri} - 1)$$
$$\frac{dE'_{qi}}{dt} = -\frac{1}{T'_{d0}}\left(E_{fdi} - E'_{qi} - (X_{di} - X'_{di})I_{gdi}\right)$$
$$\frac{dE_{fdi}}{dt} = \frac{K_{Ai}}{T_{Ei} + K_{Ai}K_{Fi}}\left(V_{refi} + V_{Si} - E_{ti}\right) - \frac{K_{Ei}}{T_{Ei} + K_{Ai}K_{Fi}}E_{fdi} \quad \textbf{(1)}$$

Where:
ω_r : Rotor angular velocity (pu);
δ : Rotor angular position in electrical radians relative to a reference which rotates at synchronous speed $\omega_0 = 2\pi f_0$ in rad/s;
f_0: Base frequency (Hz);
E'_q : Voltage proportional to the forward component of the rotor flux (pu);
E_{fd} : Voltage proportional to the forward excitation voltage (pu);
E_t : Voltages at the generator nodes (pu);
T_m : Mechanical torque (pu);
T_e : Electromagnetic torque (pu);
I_{gd} : Forward component of the generator stator current (pu);
V_S : Additional signal (pu);
V_{ref} : Reference voltage (pu);
d/dt: Time derivative.
In pu, the power has the same value as the torque.

- Relationship between Interconnected Machines in the Network

The current components injected by machine are:

$$i_{di} = \sum_{j=1}^{m} Y_{fij}\left(-\sin(\beta_{ij} + \delta_{ij})\,E'_{qj} + (X_{qj} - X'_{dj})\cos(\beta_{ij} + \delta_{ij})\,I_{qj}\right)$$
$$i_{qi} = \sum_{j=1}^{m} Y_{fij}\left(\cos(\beta_{ij} + \delta_{ij})\,E'_{qj} + (X_{qj} - X'_{dj})\sin(\beta_{ij} + \delta_{ij})\,I_{qj}\right) \quad \textbf{(2)}$$

With:
$\delta_{ij} = \delta_j - \delta_i$; $\bar{Y}_{fij} = Y_{fij}e^{j\beta_{ij}}$

- Auxiliary Equations:

$$E_{tdi} = X_{qi}I_{qi}$$
$$E_{tqi} = E'_{qi} - X'_{di}I_{di}$$
$$E_{ti}^2 = E_{tdi}^2 + E_{tqi}^2$$
$$T_{ei} = P_{ei} = Re(\bar{I}_{gi}.\bar{E}_{ti}) = E_{tdi}.I_{di} + E_{tqi}.I_{qi}$$
$$P_{ei} = \sum_{j=1}^{m}\Big(Y_{fij}\Big[E'_{q0j}\Big(E_{td0i}\Big(-\sin\big(\beta_{ij} + (\delta_j - \delta_i)\big)\Big) + E_{tq0i}\Big(\cos\big(\beta_{ij} + (\delta_j - \delta_i)\big)\Big)\Big) + (X_{qj} - X'_{dj})I_{q0j}\Big(E_{td0i}\cos\big(\beta_{ij} + (\delta_j - \delta_i)\big) + E_{tq0i}\sin\big(\beta_{ij} + (\delta_j - \delta_i)\big)\Big)\Big]\Big) \quad \textbf{(3)}$$

II-3-2. Global Linear State-Space Model

To obtain a linear state-space model, the nonlinear model is linearized around a chosen operating point. The resulting model is [3][8]:

$$\Delta\dot{\delta}_i = \omega_0.\Delta\omega_{ri}$$

International Journal of Advances in Engineering and Management (IJAEM)
Volume 8, Issue 1 Jan. 2026, pp: 375-390 www.ijaem.net ISSN: 2395-5252

$$\Delta\dot{\omega}_{ri} = -\frac{K_{Di}}{M_i}.\Delta\omega_{ri} - \frac{1}{M_i}\sum_{j=1}^{m} K_{1ij}\Delta\delta_j - \frac{1}{M_i}\sum_{j=1}^{m} K_{2ij}\Delta E'_{qj} + \frac{1}{M_i}\Delta P_{mi}$$

$$\Delta\dot{E}'_{qi} = -\frac{1}{T'_{d0i}}\sum_{j=1}^{m} K_{4ij}\Delta\delta_j - \frac{1}{T'_{d0i}}\sum_{j=1}^{m}\frac{1}{K_{3ij}}\Delta E'_{qi} + \frac{1}{T'_{d0i}}\Delta E_{fdi}$$

$$\Delta\dot{E}_{fdi} = \frac{K_{Ai}}{T_{Ei}+K_{Ai}K_{Fi}}\left(-\sum_{j=1}^{m} K_{5ij}\Delta\delta_j - \sum_{j=1}^{m} K_{6ij}\Delta E'_{qj} - \frac{K_{Ei}}{K_{Ai}}\Delta E_{fdi} + \Delta V_{refi} + \Delta V_{Si}\right) \quad \textbf{(4)}$$

With:

For $i = 1 \dots m$ and $j = 1 \dots m$

$$K_{1ii} = D_{ti}F_{dii} + Q_{ti}F_{qii}$$
$$K_{1ij} = D_{ti}F_{dij} + Q_{ti}F_{qij}$$
$$K_{2ii} = D_{ti}Y_{dii} + Q_{ti}Y_{qii} + I_{qi0}$$
$$K_{2ij} = D_{ti}Y_{dij} + Q_{ti}Y_{qij}$$
$$K_{3ii} = \frac{1}{1+(X_{di}-X'_{di})Y_{dii}}$$
$$K_{3ij} = \frac{1}{(X_{di}-X'_{di})Y_{dij}}$$
$$K_{4ii} = (X_{di}-X'_{di})F_{dii}$$
$$K_{4ij} = (X_{di}-X'_{di})F_{dij}$$
$$[K_5] = [D_v][X_q][F_q] - [Q_v][X'_d][F_d]$$
$$[K_6] = [D_v][X_q][Y_q] - [Q_v][X'_d][Y_d] + [Q_v]$$

Where:

$$D_{ti} = (X_{qi}-X'_{di})I_{qi0}$$
$$Q_{ti} = (X_{qi}-X'_{di})I_{di0} + E'_{qi0}$$
$$F_q = [L_q]^{-1}[P_q]$$
$$[F_d] = [P_d] + [M_d][F_q]$$
$$L_{qij} = -Y_{fij}(X_{qj}-X'_{dj})S_{ij} \quad j \neq i$$
$$L_{qii} = 1 - Y_{fii}(X_{qi}-X'_{di})S_{ii}$$
$$M_{dij} = Y_{fij}(X_{qj}-X'_{dj})C_{ij}$$
$$C_{ij} = \cos(\beta_{ij}+\delta_{ij})$$
$$S_{ij} = \sin(\beta_{ij}+\delta_{ij})$$
$$P_{dii} = -\sum_{j\neq i} P_{dij}$$
$$P_{dij} = -Y_{fij}(C_{ij}E'_{q0j} + (X_{qj}-X'_{dj})S_{ij}I_{q0j}) \quad j \neq i$$
$$P_{qii} = \sum_{j\neq i} P_{qij}$$
$$P_{qij} = -Y_{fij}(S_{ij}E'_{q0j} - (X_{qj}-X'_{dj})C_{ij}I_{q0j}) \quad j \neq i$$
$$Y_q = [L_q]^{-1}[Q_q]$$
$$[Y_d] = [Q_d] + [M_d][Y_q]$$
$$Q_{qij} = Y_{fij}C_{ij}$$
$$Q_{dij} = -Y_{fij}S_{ij}$$
$$[D_v] = [E_{t0}]^{-1}[E_{td0}]$$
$$[Q_v] = [E_{t0}]^{-1}[E_{tq0}]$$

In the equations, E_{t0}, E_{td0}, E_{tq0}, D_v and Q_v are diagonal matrices, while ΔE_{td}, ΔE_{tq} are vector matrices.

The voltages E_{t0}, E_{td0}, E_{tq0} are scalar values of the terminal voltage and its projections on the (di, qi) axes.

Remark: From equation **(4)**, we observe that generator i varies as a function of generators j. This means that when disturbances affect generator j, generator i is also impacted if its regulation system is not properly coordinated. Therefore, inter-machine interactions negatively affect system stability. In this paper, our approach aims to suppress these interactions in order to obtain a stable and robust system. We therefore propose the following methods.

III. METHODOLOGY

The global linear model of the power network clearly highlights the interactions among all generators. Each generator's dynamics depend on its local variables and on global variables linked to other generators. Hence, each generator control law consists of a local control specific to that generator and a global control that eliminates interactions.

III-1. Control Structure

The global regulator eliminates or attenuates interactions by decoupling each generator from the others. Removing these disturbances increases local controller performance and therefore improves overall grid stability. Figure 3 shows the control scheme of the three-generator network (G_1, G_2, G_3). The global controller uses measurements from the generators to build a global control action that operates simultaneously with each generator's local control.

International Journal of Advances in Engineering and Management (IJAEM)
Volume 8, Issue 1 Jan. 2026, pp: 375-390 www.ijaem.net ISSN: 2395-5252

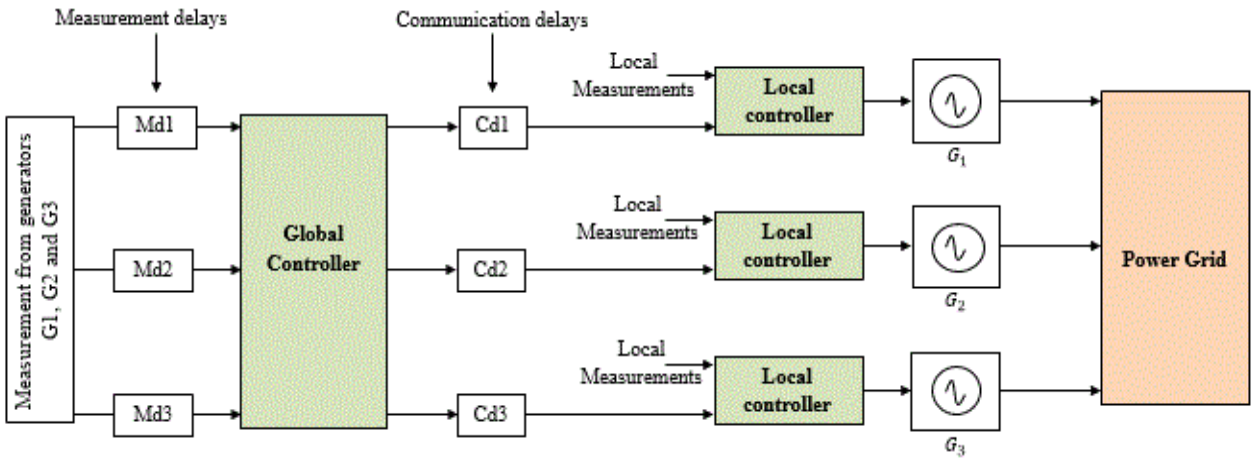

Figure 3: Control structure of the three-generator network

In this study, communication and measurement delays are neglected; therefore, Mdi and Cdi are zero.

The global controller's role is to decouple generators so that each generator's behavior depends only on local variables. Each generator controls voltage through the excitation system (E_{fdi}) and controls frequency through the mechanical torque T_{mi}.

We decompose the control inputs into local terms (E_{fdi}^L, V_{si}^L and T_{mi}^L) produced by the local regulator and global terms (E_{fdi}^G, V_{si}^G and P_{mi}^G) produced by the global regulator (Figure 4).

$$E_{fdi} = E_{fdi}^L + E_{fdi}^G$$
$$V_{si} = V_{si}^L + V_{si}^G$$
$$P_{mi} = P_{mi}^L + P_{mi}^G \quad \textbf{(5)}$$

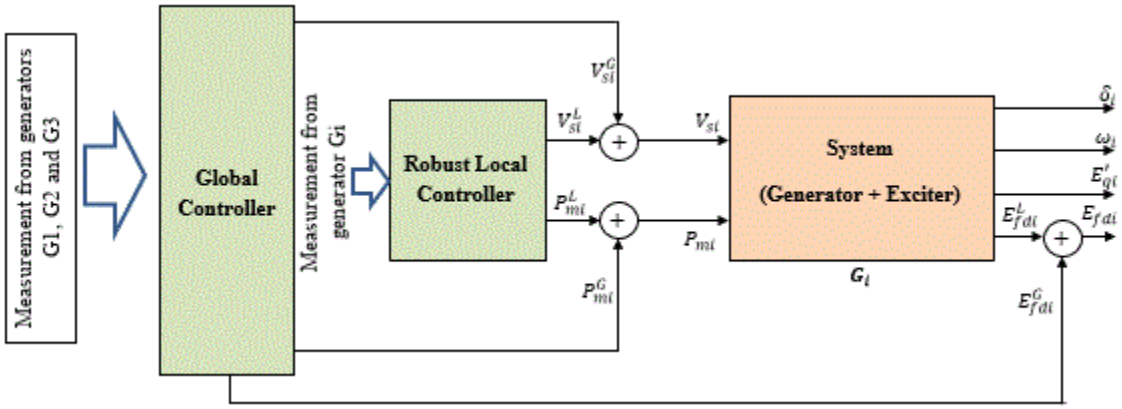

Figure 4: Control of G_i : local controller with global controller signals

III-2. Synthesis of the Global Control Law

Our goal is to compute new control actions E_{fdi}^G, V_{si}^G and P_{mi}^G in order to eliminate interactions between generators. Once interactions are removed, the voltage and rotor-speed dynamics depend only on the local parameters of generator i independently of generators j. This decoupling increases local regulator performance and improves overall grid stability.

The controller equations consist in finding global control laws E_{fdi}^G, V_{si}^G and P_{mi}^G. We replace E_{fdi}, V_{si} and P_{mi} in equation (4) by:

$$E_{fdi} = \Delta E_{fdi}^L + \Delta E_{fdi}^G$$
$$V_{si} = \Delta V_{si}^L + \Delta V_{si}^G$$
$$P_{mi} = \Delta P_{mi}^L + \Delta P_{mi}^G \quad \textbf{(6)}$$

And we obtain:

$$\Delta\dot{\delta}_1 = \omega_0.\Delta\omega_{r1}$$
$$\Delta\dot{\delta}_2 = \omega_0.\Delta\omega_{r2}$$
$$\Delta\dot{\delta}_3 = \omega_0.\Delta\omega_{r3}$$

International Journal of Advances in Engineering and Management (IJAEM)
Volume 8, Issue 1 Jan. 2026, pp: 375-390 www.ijaem.net ISSN: 2395-5252

$$\Delta\dot{\omega}_{r1} = -\frac{K_{D1}}{M_1}.\Delta\omega_{r1} + \frac{1}{M_1}\left(-K_{1(1,1)}\Delta\delta_1 - K_{2(1,1)}\Delta E'_{q1} + \Delta P^L_{m1}\right) + \frac{1}{M_1}\left(-K_{1(1,2)}\Delta\delta_2 - K_{1(1,3)}\Delta\delta_3 - K_{2(1,2)}\Delta E'_{q2} - K_{2(1,3)}\Delta E'_{q3} + \Delta P^G_{m1}\right)$$

$$\Delta\dot{\omega}_{r2} = -\frac{K_{D2}}{M_2}.\Delta\omega_{r2} + \frac{1}{M_2}\left(-K_{1(2,2)}\Delta\delta_2 - K_{2(2,2)}\Delta E'_{q2} + \Delta P^L_{m2}\right) + \frac{1}{M_2}\left(-K_{1(2,1)}\Delta\delta_1 - K_{1(2,3)}\Delta\delta_3 - K_{2(2,1)}\Delta E'_{q1} - K_{2(2,3)}\Delta E'_{q3} + \Delta P^G_{m2}\right)$$

$$\Delta\dot{\omega}_{r3} = -\frac{K_{D3}}{M_3}.\Delta\omega_{r3} + \frac{1}{M_3}\left(-K_{1(3,3)}\Delta\delta_3 - K_{2(3,3)}\Delta E'_{q3} + \Delta P^L_{m3}\right) + \frac{1}{M_3}\left(-K_{1(3,1)}\Delta\delta_1 - K_{1(3,2)}\Delta\delta_2 - K_{2(3,1)}\Delta E'_{q1} - K_{2(3,2)}\Delta E'_{q2} + \Delta P^G_{m3}\right)$$

$$\Delta\dot{E}'_{q1} = \frac{1}{T'_{d01}}\left(-K_{4(1,1)}\Delta\delta_1 - \frac{1}{K_{3(1,1)}}\Delta E'_{q1} + \Delta E^L_{fd1}\right) + \frac{1}{T'_{d01}}\left(-K_{4(1,2)}\Delta\delta_2 - K_{4(1,3)}\Delta\delta_3 - \frac{1}{K_{3(1,2)}}\Delta E'_{q2} - \frac{1}{K_{3(1,3)}}\Delta E'_{q3} + \Delta E^G_{fd1}\right)$$

$$\Delta\dot{E}'_{q2} = \frac{1}{T'_{d02}}\left(-K_{4(2,2)}\Delta\delta_2 - \frac{1}{K_{3(2,2)}}\Delta E'_{q2} + \Delta E^L_{fd2}\right) + \frac{1}{T'_{d02}}\left(-K_{4(2,1)}\Delta\delta_1 - K_{4(2,3)}\Delta\delta_3 - \frac{1}{K_{3(2,1)}}\Delta E'_{q1} - \frac{1}{K_{3(2,3)}}\Delta E'_{q3} + \Delta E^G_{fd2}\right)$$

$$\Delta\dot{E}'_{q3} = \frac{1}{T'_{d03}}\left(-K_{4(3,3)}\Delta\delta_3 - \frac{1}{K_{3(3,3)}}\Delta E'_{q3} + \Delta E^L_{fd3}\right) + \frac{1}{T'_{d03}}\left(-K_{4(3,1)}\Delta\delta_1 - K_{4(3,2)}\Delta\delta_2 - \frac{1}{K_{3(3,1)}}\Delta E'_{q1} - \frac{1}{K_{3(3,2)}}\Delta E'_{q2} + \Delta E^G_{fd3}\right)$$

$$\Delta\dot{E}_{fd1} = \frac{K_{A1}}{T_{E1}+K_{A1}K_{F1}}\left(-K_{5(1,1)}\Delta\delta_1 - K_{6(1,1)}\Delta E'_{q1} - \frac{K_{E1}}{K_{A1}}\Delta E_{fd1} + \Delta V^L_{s1} + \Delta V_{ref1}\right) + \frac{K_{A1}}{T_{E1}+K_{A1}K_{F1}}\left(-K_{5(1,2)}\Delta\delta_2 - K_{5(1,3)}\Delta\delta_3 - K_{6(1,2)}\Delta E'_{q2} - K_{6(1,3)}\Delta E'_{q3} - \frac{K_{E1}}{K_{A1}}\Delta E^G_{fd1} + \Delta V^G_{s1}\right)$$

$$\Delta\dot{E}_{fd2} = \frac{K_{A2}}{T_{E2}+K_{A2}K_{F2}}\left(-K_{5(2,2)}\Delta\delta_2 - K_{6(2,2)}\Delta E'_{q2} - \frac{K_{E2}}{K_{A2}}\Delta E_{fd2} + \Delta V_{ref2} + \Delta V^L_{s2}\right) + \frac{K_{A2}}{T_{E2}+K_{A2}K_{F2}}\left(-K_{5(2,1)}\Delta\delta_1 - K_{5(2,3)}\Delta\delta_3 - K_{6(2,1)}\Delta E'_{q1} - K_{6(2,3)}\Delta E'_{q3} - \frac{K_{E2}}{K_{A2}}\Delta E^G_{fd2} + \Delta V^G_{s2}\right)$$

$$\Delta\dot{E}_{fd3} = \frac{K_{A3}}{T_{E3}+K_{A3}K_{F3}}\left(-K_{5(3,3)}\Delta\delta_3 - K_{6(3,3)}\Delta E'_{q3} - \frac{K_{E3}}{K_{A3}}\Delta E_{fd3} + \Delta V_{ref3} + \Delta V^L_{s3}\right) + \frac{K_{A3}}{T_{E3}+K_{A3}K_{F3}}\left(-K_{5(3,1)}\Delta\delta_1 - K_{5(3,2)}\Delta\delta_2 - K_{6(3,1)}\Delta E'_{q1} - K_{6(3,2)}\Delta E'_{q2} - \frac{K_{E3}}{K_{A3}}\Delta E^G_{fd3} + \Delta V^G_{s3}\right)$$

(7)

To cancel the interactions due to the other generators, we choose the global regulator equations as follows:

$$\Delta P^G_{m1} = K_{1(1,2)}\Delta\delta_2 + K_{1(1,3)}\Delta\delta_3 + K_{2(1,2)}\Delta E'_{q2} + K_{2(1,3)}\Delta E'_{q3}$$

$$\Delta P^G_{m2} = K_{1(2,1)}\Delta\delta_1 + K_{1(2,3)}\Delta\delta_3 + K_{2(2,1)}\Delta E'_{q1} + K_{2(2,3)}\Delta E'_{q3}$$

International Journal of Advances in Engineering and Management (IJAEM)
Volume 8, Issue 1 Jan. 2026, pp: 375-390 www.ijaem.net ISSN: 2395-5252

$$\Delta P_{m3}^{G} = K_{1(3,1)}\Delta\delta_1 + K_{1(3,2)}\Delta\delta_2 + K_{2(3,1)}\Delta E'_{q1} + K_{2(3,2)}\Delta E'_{q2}$$
$$\Delta E_{fd1}^{G} = K_{4(1,2)}\Delta\delta_2 + K_{4(1,3)}\Delta\delta_3 + \frac{1}{K_{3(1,2)}}\Delta E'_{q2} + \frac{1}{K_{3(1,3)}}\Delta E'_{q3}$$
$$\Delta E_{fd2}^{G} = K_{1(3,1)}\Delta\delta_1 + K_{1(3,2)}\Delta\delta_2 + K_{2(3,1)}\Delta E'_{q1} + K_{2(3,2)}\Delta E'_{q2}$$
$$\Delta E_{fd3}^{G} = K_{4(3,1)}\Delta\delta_1 + K_{4(3,2)}\Delta\delta_2 + \frac{1}{K_{3(3,1)}}\Delta E'_{q1} + \frac{1}{K_{3(3,2)}}\Delta E'_{q2}$$
$$\Delta V_{s1}^{G} = K_{5(1,2)}\Delta\delta_2 + K_{5(1,3)}\Delta\delta_3 + K_{6(1,2)}\Delta E'_{q2} + K_{6(1,3)}\Delta E'_{q3} + \frac{K_{E1}}{K_{A1}}\Delta E_{fd1}^{G}$$
$$\Delta V_{s2}^{G} = K_{5(2,1)}\Delta\delta_1 + K_{5(2,3)}\Delta\delta_3 + K_{6(2,1)}\Delta E'_{q1} + K_{6(2,3)}\Delta E'_{q3} + \frac{K_{E2}}{K_{A2}}\Delta E_{fd2}^{G}$$
$$\Delta V_{s3}^{G} = K_{5(3,1)}\Delta\delta_1 + K_{5(3,2)}\Delta\delta_2 + K_{6(3,1)}\Delta E'_{q1} + K_{6(3,2)}\Delta E'_{q2} + \frac{K_{E3}}{K_{A3}}\Delta E_{fd3}^{G} \quad \textbf{(8)}$$

The remaining dynamics are then:

$$\Delta\dot{\delta}_i = \omega_0.\Delta\omega_{ri}$$
$$\Delta\dot{\omega}_{ri} = J_1^i.\Delta\omega_{ri} + J_2^i.\Delta\delta_i + J_3^i.\Delta E'_{qi} + J_4^i.\Delta P_{mi}$$
$$\Delta\dot{E}'_{qi} = K_1^i.\Delta\delta_i + K_2^i.\Delta E'_{qi} + K_3^i\Delta E_{fdi}$$
$$\Delta\dot{E}_{fdi} = L_1^i.\Delta\delta_i + L_2^i.\Delta E'_{qi} + L_3^i.\Delta E_{fdi} + L_4^i\left(\Delta V_{refi} + \Delta V_{si}\right) \quad \textbf{(9)}$$

Where:

$$J_1^i = \frac{-K_{Di}}{M_i}\ ;\ J_2^i = \frac{-K_{1(i,i)}}{M_i}\ ;\ J_3^i = \frac{-K_{2(i,i)}}{M_i}\ ;\ J_4^i = \frac{1}{M_i}$$
$$K_1^i = \frac{-K_{4(i,i)}}{T'_{d0i}}\ ;\ K_2^i = \frac{-1}{T'_{d0i}.K_{3(i,i)}}\ ;\ K_3^i = \frac{1}{T'_{d0i}}$$
$$L_1^i = \frac{-K_{Ai}.K_{5(i,i)}}{T_{Ei}+K_{Ai}K_{Fi}}\ ;\ L_2^i = \frac{-K_{Ai}.K_{6(i,i)}}{T_{Ei}+K_{Ai}K_{Fi}}\ ;\ L_3^i = \frac{-K_{Ei}}{T_{Ei}+K_{Ai}K_{Fi}}\ ;\ L_4^i = \frac{K_{Ai}}{T_{Ei}+K_{Ai}K_{Fi}}$$

$i = 1, 2$ and 3 : machine indices.

III-3. Synthesis of the Local Controller

Local controller synthesis for each generator is carried out from the remaining dynamics equation **(9)** via control H∞.

III-3-1. Nominal system

The detailed block diagram for each generator is:

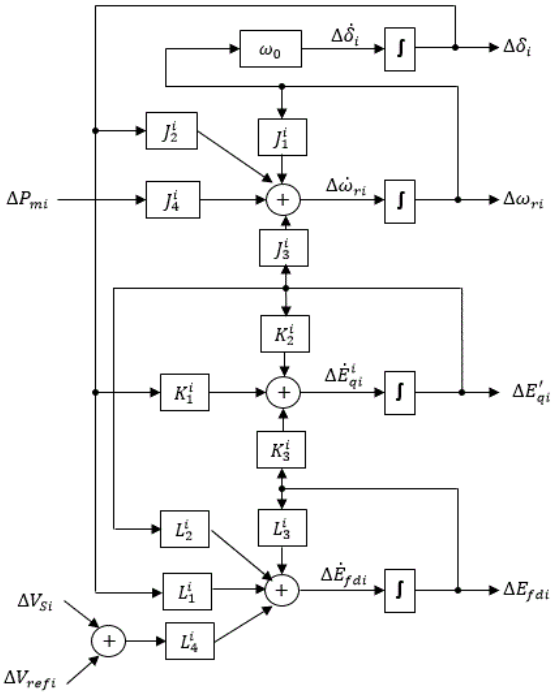

Figure 5: Block Diagram of the Local Nominal System

Table 6: The poles of the system

system	Poles
G_1	– 1.4932 + 1.8813i 0.9015 – 1.7325i 0.7375 + 0.3974i – 0.9828 – 0.2986i
G_2	– 4.1788 + 4.5251i 3.0686 – 3.8859i 0.3416 + 0.9360i – 0.8124 – 0.8479i
G_3	– 3.8528 + 4.7552i 2.1768 – 4.2251i 1.1267 + 0.3242i – 1.4765 – 0.1932i

The pole results indicate that G_1, G_2, and G_3 are unstable.

III-3-2. System Uncertainty

In this study, system parameters are subject to uncertainty. Each uncertain coefficient $\tilde{p}_i$ is modeled as [12][13]:

$$\tilde{p}_i = p_i + w_{pi} \quad \textbf{(10)}$$

Where:

p_i : Nominal value of the considered parameter;

w_{p_i} : Variation coefficient of p_i

The parameters sensitive to disturbances are: K_1, K_2, K_3, K_4, K_5 and K_6. Therefore:

$$\tilde{K}_1 = K_1 + w_{K_1} \quad , \quad w_{K_1} = 6\ \%$$

International Journal of Advances in Engineering and Management (IJAEM)
Volume 8, Issue 1 Jan. 2026, pp: 375-390 www.ijaem.net ISSN: 2395-5252

$$\tilde{K}_2 = K_2 + w_{K_2} \quad , \quad w_{K_2} = 6\,\%$$
$$\tilde{K}_3 = K_3 + w_{K_3} \quad , \quad w_{K_3} = 6\,\%$$
$$\tilde{K}_4 = K_4 + w_{K_4} \quad , \quad w_{K_4} = 6\,\%$$
$$\tilde{K}_5 = K_5 + w_{K_5} \quad , \quad w_{K_5} = 6\,\%$$
$$\tilde{K}_6 = K_6 + w_{K_6} \quad , \quad w_{K_6} = 6\,\%$$

III-3-3. Weighting Functions

The synthesis is based on introducing three weighting functions $W_1(s)$, $W_2(s)$ and $W_3(s)$ for each system.

Table 7: Weighting Functions

System	$W_1(s)$	$W_2(s)$	$W_3(s)$
G_1	$\frac{10^{-10}(s+5)}{s^2+10^2\,s+10^3}$	$\frac{10^{-7}(s^2-8.039\times10^{-14}\,s+10^{-2})}{s^2+500\,s+10^6}$	$\frac{10^{-6}(2\,s+5)}{s^2+s+1}$
G_2	$\frac{10^{-10}(s+5)}{s^2+10^4\,s+10^3}$	$\frac{10^{-15}(s^2-5.551\times10^{-17}\,s+10^{-2})}{s^2+0.5\,s+0.1}$	$\frac{10^{-19}(2\,s+5)}{s^2+10^{-3}\,s+1}$
G_3	$\frac{10^{-10}(s+5)}{s^2+10^2\,s+10^3}$	$\frac{10^{-7}(s^2+8.039\times10^{-14}\,s+10^{-2})}{s^2+500\,s+10^6}$	$\frac{10^{-6}(2\,s+5)}{s^2+s+1}$

The choice of the above weightings constrains the system to satisfy the following inequalities over the entire frequency range [12][13]:

$$\begin{cases} \|W_1 S\|_\infty < 1 \\ \|W_2 KS\|_\infty < 1 \\ \|W_3 T\|_\infty < 1 \end{cases} \qquad \textbf{(11)}$$

With

$$\begin{cases} S = (I+GK)^{-1} \\ KS = K(I+GK)^{-1} \\ T = GKS \end{cases}$$

III-3-4. Controller Design via H∞

Figure 6 presents the block diagram of the robust controller synthesis [12][13].

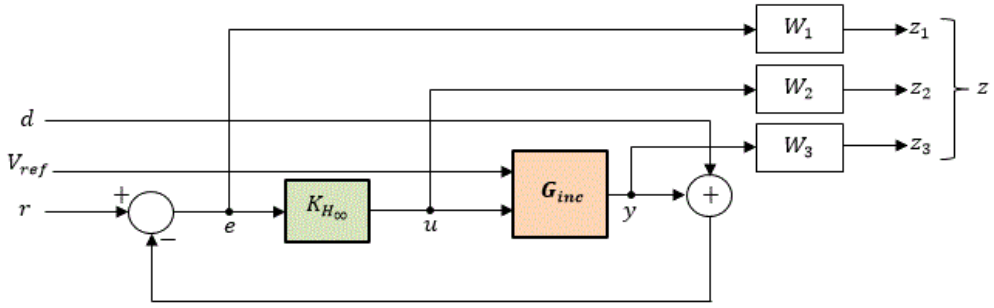

Figure 6: Block diagram of the robust synthesis

Where:
K_{H_∞} : Controller H∞;
G_{inc}: Perturbed system;
u : System control vector $[\Delta P_m \;\; \Delta V_s]^T$;
y : System outputs vector $[\Delta\delta \; \Delta\omega_r \; \Delta E'_q \; \Delta E_{fd}]^T$;
d : Disturbance on the system outputs $[d_1\; d_2\; d_3\; d_4]^T$;
r : Setpoints $[\delta_{ref} \; \omega_{ref} \; E'_{q\_ref} \; E_{fd\_ref}]^T$.

III-3-5. Local Regulator

From the simulation, the obtained local regulator for each generator is written in the form:

$$K_{H_\infty} = \begin{bmatrix} K_{11} & K_{12} & K_{13} & K_{14} \\ K_{21} & K_{22} & K_{23} & K_{24} \end{bmatrix} \qquad \textbf{(25)}$$

IV. RESULTS AND DISCUSSION

IV-1. Stability of the Perturbed Local System in Closed Loop with K_{H_∞} : Nominal System Performance

Table 8: H∞ Norm of Weighted Sensitivity Functions W_1S, W_2KS and W_3T

	Transfer Function	H-∞ Norm	$\omega_{pic}(rad/s)$

International Journal of Advances in Engineering and Management (IJAEM)
Volume 8, Issue 1 Jan. 2026, pp: 375-390 www.ijaem.net ISSN: 2395-5252

G_1	W_1S	1.6096×10^{-12}	11.8578
	W_2KS	5.5303×10^{-8}	132.3035
	W_3T	7.1606×10^{-6}	0.7071
G_2	W_1S	1.6824×10^{-13}	0.3272
	W_2KS	3.3419×10^{-15}	31.8003
	W_3T	7.7884×10^{-16}	1.0000
G_3	W_1S	1.6096×10^{-12}	11.8578
	W_2KS	5.5303×10^{-8}	132.3035
	W_3T	7.1606×10^{-6}	0.7071

Table-8 represent the H∞ norm response of the transfer functions W_1S, W_2KS and W_3T for each system. It is observed that all norms are less than 1, meaning the performance condition of the nominal system for the H∞ synthesis problem is fully satisfied.

IV-.2-1. Result using μ-analysis

For G_1

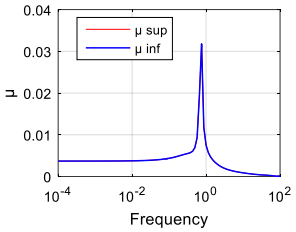

$\max(\mu_{Sup}) = 0.0318 ; \max(\mu_{\text{Inf}}) = 0.0318$

Figure 7: μ-analysis of the closed-loop system with $K_{H\infty_1}$

For G_2

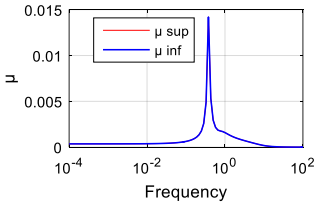

$\max(\mu_{Sup}) = 0.0142 ; \max(\mu_{\text{Inf}}) = 0.0142$

Figure 8: μ-analysis of the closed-loop system with $K_{H\infty_2}$

For G_3

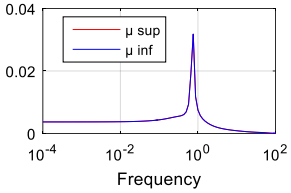

$\max(\mu_{Sup}) = 0.0318; \max(\mu_{\text{Inf}}) = 0.0318$

Figure 9: μ-analysis of the closed-loop system with $K_{H\infty_3}$

Figures 7 – 9 show the μ curve of the closed-loop system with the controller, including lower and upper bounds of the structured singular value. The maximum μ values are well below 1, indicating that:
the corrected system is robustly stable and robustly performant with respect to the introduced parametric uncertainties; it satisfies expected robustness margins under the μ-analysis framework.

4.2.2 Result using MATLAB commands "robuststab" and "robustperf"

- Robust stability: robuststab

International Journal of Advances in Engineering and Management (IJAEM)
Volume 8, Issue 1 Jan. 2026, pp: 375-390 www.ijaem.net ISSN: 2395-5252

For G_1

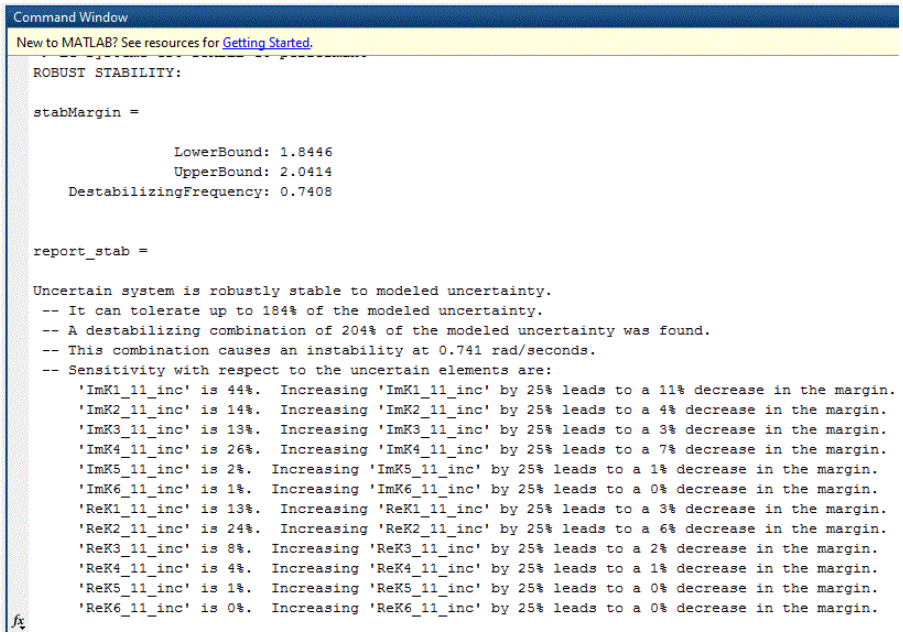

```
Command Window
New to MATLAB? See resources for Getting Started.

ROBUST STABILITY:

stabMargin =

               LowerBound: 1.8446
               UpperBound: 2.0414
    DestabilizingFrequency: 0.7408


report_stab =

Uncertain system is robustly stable to modeled uncertainty.
 -- It can tolerate up to 184% of the modeled uncertainty.
 -- A destabilizing combination of 204% of the modeled uncertainty was found.
 -- This combination causes an instability at 0.741 rad/seconds.
 -- Sensitivity with respect to the uncertain elements are:
     'ImK1_11_inc' is 44%.  Increasing 'ImK1_11_inc' by 25% leads to a 11% decrease in the margin.
     'ImK2_11_inc' is 14%.  Increasing 'ImK2_11_inc' by 25% leads to a 4% decrease in the margin.
     'ImK3_11_inc' is 13%.  Increasing 'ImK3_11_inc' by 25% leads to a 3% decrease in the margin.
     'ImK4_11_inc' is 26%.  Increasing 'ImK4_11_inc' by 25% leads to a 7% decrease in the margin.
     'ImK5_11_inc' is 2%.  Increasing 'ImK5_11_inc' by 25% leads to a 1% decrease in the margin.
     'ImK6_11_inc' is 1%.  Increasing 'ImK6_11_inc' by 25% leads to a 0% decrease in the margin.
     'ReK1_11_inc' is 13%.  Increasing 'ReK1_11_inc' by 25% leads to a 3% decrease in the margin.
     'ReK2_11_inc' is 24%.  Increasing 'ReK2_11_inc' by 25% leads to a 6% decrease in the margin.
     'ReK3_11_inc' is 8%.  Increasing 'ReK3_11_inc' by 25% leads to a 2% decrease in the margin.
     'ReK4_11_inc' is 4%.  Increasing 'ReK4_11_inc' by 25% leads to a 1% decrease in the margin.
     'ReK5_11_inc' is 1%.  Increasing 'ReK5_11_inc' by 25% leads to a 0% decrease in the margin.
     'ReK6_11_inc' is 0%.  Increasing 'ReK6_11_inc' by 25% leads to a 0% decrease in the margin.
```

For G_2

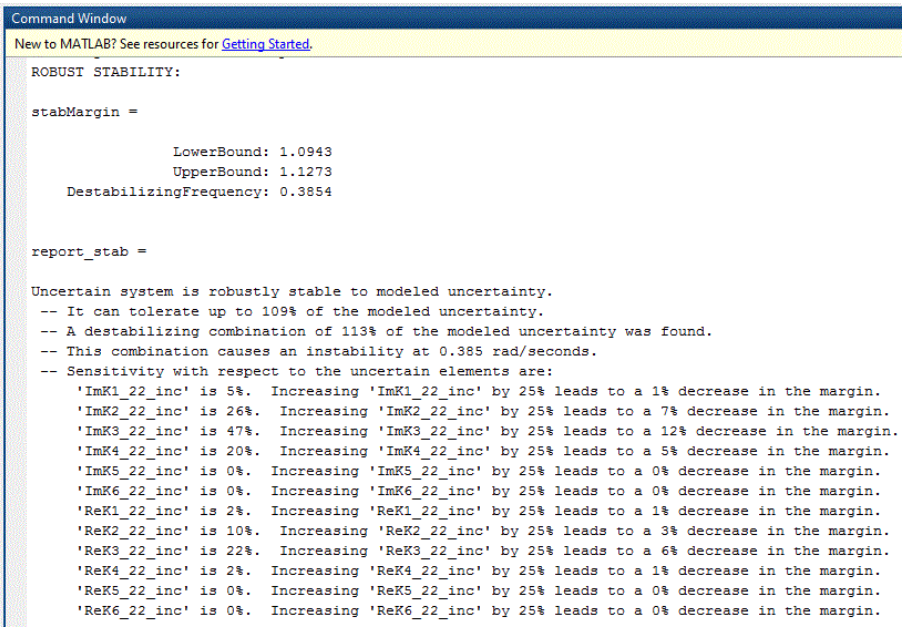

```
Command Window
New to MATLAB? See resources for Getting Started.

ROBUST STABILITY:

stabMargin =

               LowerBound: 1.0943
               UpperBound: 1.1273
    DestabilizingFrequency: 0.3854


report_stab =

Uncertain system is robustly stable to modeled uncertainty.
 -- It can tolerate up to 109% of the modeled uncertainty.
 -- A destabilizing combination of 113% of the modeled uncertainty was found.
 -- This combination causes an instability at 0.385 rad/seconds.
 -- Sensitivity with respect to the uncertain elements are:
     'ImK1_22_inc' is 5%.  Increasing 'ImK1_22_inc' by 25% leads to a 1% decrease in the margin.
     'ImK2_22_inc' is 26%.  Increasing 'ImK2_22_inc' by 25% leads to a 7% decrease in the margin.
     'ImK3_22_inc' is 47%.  Increasing 'ImK3_22_inc' by 25% leads to a 12% decrease in the margin.
     'ImK4_22_inc' is 20%.  Increasing 'ImK4_22_inc' by 25% leads to a 5% decrease in the margin.
     'ImK5_22_inc' is 0%.  Increasing 'ImK5_22_inc' by 25% leads to a 0% decrease in the margin.
     'ImK6_22_inc' is 0%.  Increasing 'ImK6_22_inc' by 25% leads to a 0% decrease in the margin.
     'ReK1_22_inc' is 2%.  Increasing 'ReK1_22_inc' by 25% leads to a 1% decrease in the margin.
     'ReK2_22_inc' is 10%.  Increasing 'ReK2_22_inc' by 25% leads to a 3% decrease in the margin.
     'ReK3_22_inc' is 22%.  Increasing 'ReK3_22_inc' by 25% leads to a 6% decrease in the margin.
     'ReK4_22_inc' is 2%.  Increasing 'ReK4_22_inc' by 25% leads to a 1% decrease in the margin.
     'ReK5_22_inc' is 0%.  Increasing 'ReK5_22_inc' by 25% leads to a 0% decrease in the margin.
     'ReK6_22_inc' is 0%.  Increasing 'ReK6_22_inc' by 25% leads to a 0% decrease in the margin.
```

International Journal of Advances in Engineering and Management (IJAEM)
Volume 8, Issue 1 Jan. 2026, pp: 375-390 www.ijaem.net ISSN: 2395-5252

For G_3

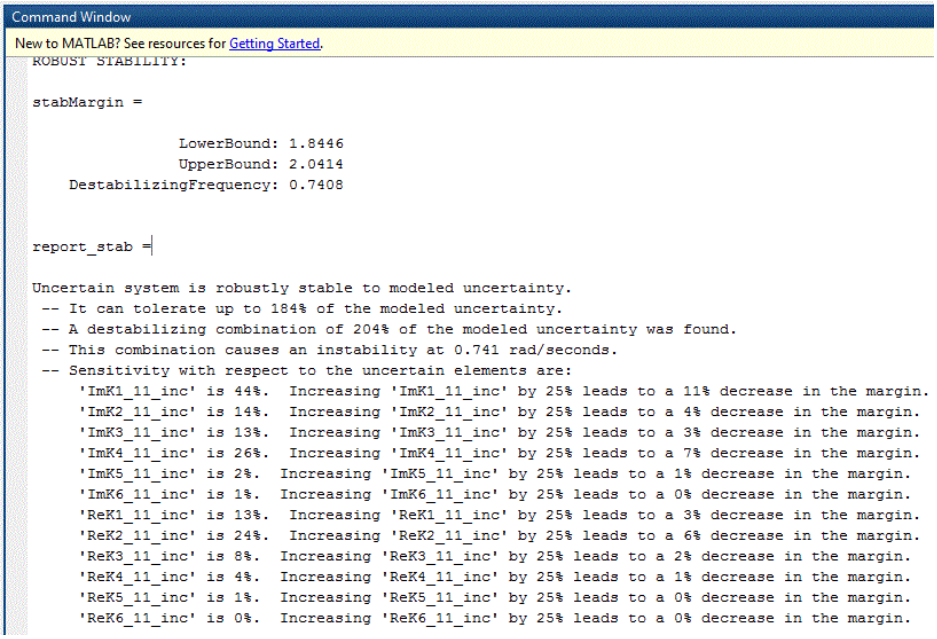

```
Command Window
New to MATLAB? See resources for Getting Started.
ROBUST STABILITY:

stabMargin =

               LowerBound: 1.8446
               UpperBound: 2.0414
    DestabilizingFrequency: 0.7408


report_stab =

Uncertain system is robustly stable to modeled uncertainty.
 -- It can tolerate up to 184% of the modeled uncertainty.
 -- A destabilizing combination of 204% of the modeled uncertainty was found.
 -- This combination causes an instability at 0.741 rad/seconds.
 -- Sensitivity with respect to the uncertain elements are:
     'ImK1_11_inc' is 44%.  Increasing 'ImK1_11_inc' by 25% leads to a 11% decrease in the margin.
     'ImK2_11_inc' is 14%.  Increasing 'ImK2_11_inc' by 25% leads to a 4% decrease in the margin.
     'ImK3_11_inc' is 13%.  Increasing 'ImK3_11_inc' by 25% leads to a 3% decrease in the margin.
     'ImK4_11_inc' is 26%.  Increasing 'ImK4_11_inc' by 25% leads to a 7% decrease in the margin.
     'ImK5_11_inc' is 2%.  Increasing 'ImK5_11_inc' by 25% leads to a 1% decrease in the margin.
     'ImK6_11_inc' is 1%.  Increasing 'ImK6_11_inc' by 25% leads to a 0% decrease in the margin.
     'ReK1_11_inc' is 13%.  Increasing 'ReK1_11_inc' by 25% leads to a 3% decrease in the margin.
     'ReK2_11_inc' is 24%.  Increasing 'ReK2_11_inc' by 25% leads to a 6% decrease in the margin.
     'ReK3_11_inc' is 8%.  Increasing 'ReK3_11_inc' by 25% leads to a 2% decrease in the margin.
     'ReK4_11_inc' is 4%.  Increasing 'ReK4_11_inc' by 25% leads to a 1% decrease in the margin.
     'ReK5_11_inc' is 1%.  Increasing 'ReK5_11_inc' by 25% leads to a 0% decrease in the margin.
     'ReK6_11_inc' is 0%.  Increasing 'ReK6_11_inc' by 25% leads to a 0% decrease in the margin.
```

- Robust performance: robustperf

For G_1

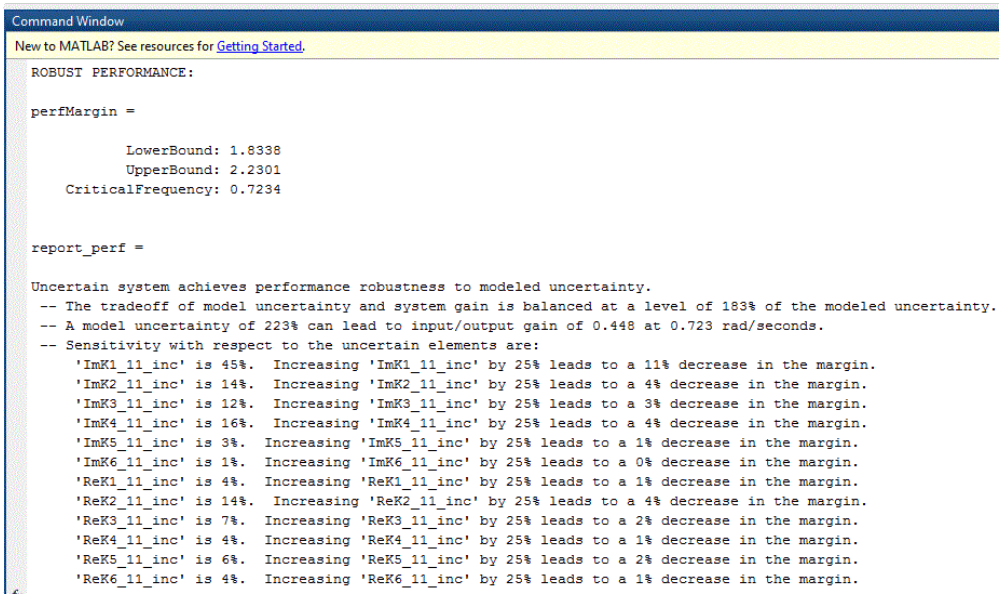

```
Command Window
New to MATLAB? See resources for Getting Started.
ROBUST PERFORMANCE:

perfMargin =

          LowerBound: 1.8338
          UpperBound: 2.2301
    CriticalFrequency: 0.7234


report_perf =

Uncertain system achieves performance robustness to modeled uncertainty.
 -- The tradeoff of model uncertainty and system gain is balanced at a level of 183% of the modeled uncertainty.
 -- A model uncertainty of 223% can lead to input/output gain of 0.448 at 0.723 rad/seconds.
 -- Sensitivity with respect to the uncertain elements are:
     'ImK1_11_inc' is 45%.  Increasing 'ImK1_11_inc' by 25% leads to a 11% decrease in the margin.
     'ImK2_11_inc' is 14%.  Increasing 'ImK2_11_inc' by 25% leads to a 4% decrease in the margin.
     'ImK3_11_inc' is 12%.  Increasing 'ImK3_11_inc' by 25% leads to a 3% decrease in the margin.
     'ImK4_11_inc' is 16%.  Increasing 'ImK4_11_inc' by 25% leads to a 4% decrease in the margin.
     'ImK5_11_inc' is 3%.  Increasing 'ImK5_11_inc' by 25% leads to a 1% decrease in the margin.
     'ImK6_11_inc' is 1%.  Increasing 'ImK6_11_inc' by 25% leads to a 0% decrease in the margin.
     'ReK1_11_inc' is 4%.  Increasing 'ReK1_11_inc' by 25% leads to a 1% decrease in the margin.
     'ReK2_11_inc' is 14%.  Increasing 'ReK2_11_inc' by 25% leads to a 4% decrease in the margin.
     'ReK3_11_inc' is 7%.  Increasing 'ReK3_11_inc' by 25% leads to a 2% decrease in the margin.
     'ReK4_11_inc' is 4%.  Increasing 'ReK4_11_inc' by 25% leads to a 1% decrease in the margin.
     'ReK5_11_inc' is 6%.  Increasing 'ReK5_11_inc' by 25% leads to a 2% decrease in the margin.
     'ReK6_11_inc' is 4%.  Increasing 'ReK6_11_inc' by 25% leads to a 1% decrease in the margin.
```

International Journal of Advances in Engineering and Management (IJAEM)
Volume 8, Issue 1 Jan. 2026, pp: 375-390 www.ijaem.net ISSN: 2395-5252

For G_2

```
Command Window
New to MATLAB? See resources for Getting Started.

ROBUST PERFORMANCE:

perfMargin =

          LowerBound: 1.0943
          UpperBound: 173.2946
    CriticalFrequency: 0.3759


report_perf =

Uncertain system achieves performance robustness to modeled uncertainty.
 -- The tradeoff of model uncertainty and system gain is balanced at a level of 109% of the modeled uncertainty.
 -- A model uncertainty of 1.73e+04% can lead to input/output gain of 0.00577 at 0.376 rad/seconds.
 -- Sensitivity with respect to the uncertain elements are:
     'ImK1_22_inc' is 5%.  Increasing 'ImK1_22_inc' by 25% leads to a 1% decrease in the margin.
     'ImK2_22_inc' is 23%.  Increasing 'ImK2_22_inc' by 25% leads to a 6% decrease in the margin.
     'ImK3_22_inc' is 47%.  Increasing 'ImK3_22_inc' by 25% leads to a 12% decrease in the margin.
     'ImK4_22_inc' is 20%.  Increasing 'ImK4_22_inc' by 25% leads to a 5% decrease in the margin.
     'ImK5_22_inc' is 0%.  Increasing 'ImK5_22_inc' by 25% leads to a 0% decrease in the margin.
     'ImK6_22_inc' is 0%.  Increasing 'ImK6_22_inc' by 25% leads to a 0% decrease in the margin.
     'ReK1_22_inc' is 2%.  Increasing 'ReK1_22_inc' by 25% leads to a 1% decrease in the margin.
     'ReK2_22_inc' is 10%.  Increasing 'ReK2_22_inc' by 25% leads to a 3% decrease in the margin.
     'ReK3_22_inc' is 22%.  Increasing 'ReK3_22_inc' by 25% leads to a 6% decrease in the margin.
     'ReK4_22_inc' is 3%.  Increasing 'ReK4_22_inc' by 25% leads to a 1% decrease in the margin.
     'ReK5_22_inc' is 0%.  Increasing 'ReK5_22_inc' by 25% leads to a 0% decrease in the margin.
     'ReK6_22_inc' is 0%.  Increasing 'ReK6_22_inc' by 25% leads to a 0% decrease in the margin.
```

For G_3

```
Command Window
New to MATLAB? See resources for Getting Started.

ROBUST PERFORMANCE:

perfMargin =

          LowerBound: 1.8338
          UpperBound: 2.2301
    CriticalFrequency: 0.7234


report_perf =

Uncertain system achieves performance robustness to modeled uncertainty.
 -- The tradeoff of model uncertainty and system gain is balanced at a level of 183% of the modeled uncertainty.
 -- A model uncertainty of 223% can lead to input/output gain of 0.448 at 0.723 rad/seconds.
 -- Sensitivity with respect to the uncertain elements are:
     'ImK1_11_inc' is 45%.  Increasing 'ImK1_11_inc' by 25% leads to a 11% decrease in the margin.
     'ImK2_11_inc' is 14%.  Increasing 'ImK2_11_inc' by 25% leads to a 4% decrease in the margin.
     'ImK3_11_inc' is 12%.  Increasing 'ImK3_11_inc' by 25% leads to a 3% decrease in the margin.
     'ImK4_11_inc' is 16%.  Increasing 'ImK4_11_inc' by 25% leads to a 4% decrease in the margin.
     'ImK5_11_inc' is 3%.  Increasing 'ImK5_11_inc' by 25% leads to a 1% decrease in the margin.
     'ImK6_11_inc' is 1%.  Increasing 'ImK6_11_inc' by 25% leads to a 0% decrease in the margin.
     'ReK1_11_inc' is 4%.  Increasing 'ReK1_11_inc' by 25% leads to a 1% decrease in the margin.
     'ReK2_11_inc' is 14%.  Increasing 'ReK2_11_inc' by 25% leads to a 4% decrease in the margin.
     'ReK3_11_inc' is 7%.  Increasing 'ReK3_11_inc' by 25% leads to a 2% decrease in the margin.
     'ReK4_11_inc' is 4%.  Increasing 'ReK4_11_inc' by 25% leads to a 1% decrease in the margin.
     'ReK5_11_inc' is 6%.  Increasing 'ReK5_11_inc' by 25% leads to a 2% decrease in the margin.
     'ReK6_11_inc' is 4%.  Increasing 'ReK6_11_inc' by 25% leads to a 1% decrease in the margin.
```

From the displayed results, G1, G2, and G3 are robustly stable and robustly performant.

V. TESTING THE EFFECTIVENESS OF THE REGULATORS

To judge the effectiveness of our regulator, we will test a network fault from Figure 10: a short-circuit at bus 1 and 3 for a duration of one second. Assume this network is equipped with a protection system. Therefore, the effect of the short-circuit at nodes 1 and 3 does not reach the other nodes. In this section, we will observe the behavior of our system facing this fault.

International Journal of Advances in Engineering and Management (IJAEM)
Volume 8, Issue 1 Jan. 2026, pp: 375-390 www.ijaem.net ISSN: 2395-5252

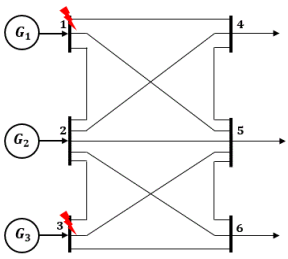

Figure 10: Network with Short-Circuit Fault

V-1. Behavior of G_1 and G_3

V-1-1. Behavior Without Fault

In this case, the disturbance inputs d_1, d_2, d_3, and d_4 are assumed to be zero. Here are the system output signals.

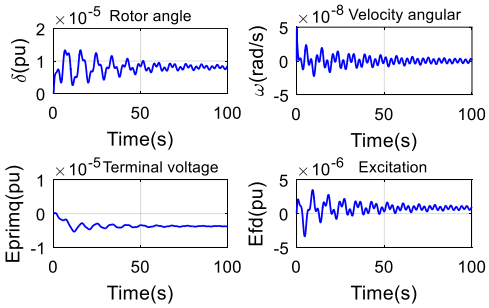

Figure 11: Impulse Response of System G_1 without fault

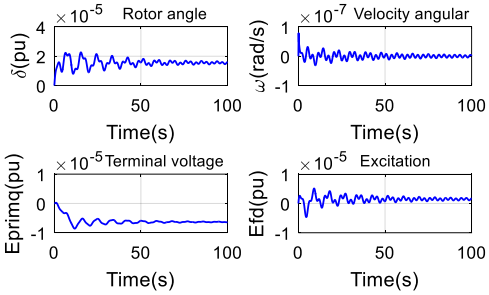

Figure 12: Impulse Response of System G_3 without fault

V-1-2. Behavior With Fault

In this case, we assume that the effect of disturbances due to the short-circuit on our system is on the order of ten times the nominal value. Here are the system output signals.

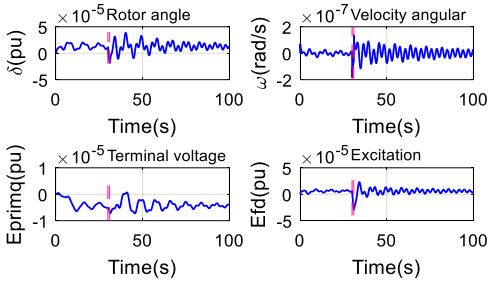

Figure 13: Impulse Response of System G_1 with fault

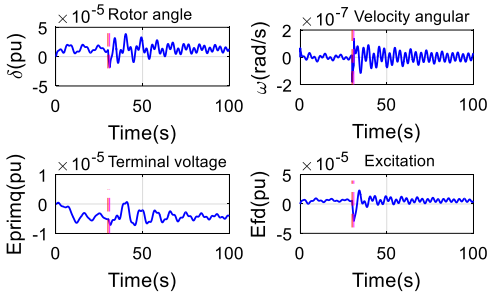

Figure 14: Impulse Response of System G_3 with fault

V-3. Interpretation of Results

In Figures (11-12) and (13-14), red lines indicate the fault instant. The controller performs well even under fault conditions: after the disturbance, each parameter signal (δ, ω, E'_q and E_{fd}) gradually converges toward the stabilizing point. These results demonstrate the robustness of the controller under disturbances.

VI. COMPARATIVE ANALYSIS WITH STATIC STATE FEEDBACK CONTROL

To assess the originality and effectiveness of our study, we will compare the result obtained by N. Abu-Tabak [3] with our own. The table below presents this comparison.

Table 9: Comparative analysis of the cascaded control and the static state-feedback control proposed by N. Abu-Tabak regarding the stability of the Multi-Machine Power Network

Method	Cascaded Control (Global and Local)	Static State-Feedback Control and Luenberger Observer (N. Abu-Tabak)
Controller synthesis method	• Elimination of interactions between machines for the synthesis of the global controller. • H∞ control for the synthesis of the local controller.	The controller and observer gains are computed by minimizing a quadratic criterion, using the LMI method to enforce pole placement and The Rosenbrock method to optimize the gains obtained from the LMI procedure.

Network used	Multi-Machine Power Network with three synchronous machine, three loads, and six buses.	Multi-Machine Power Network with three synchronous machine, four loads, and five buses.
Simulation Results of the Perturbed Closed-Loop System	• State variables are well damped but still show slight fluctuations. • The amplitude is very small, indicating good system behavior under disturbances. • The effect of output disturbances is minimized, confirming system robustness. • The settling time is around 100 s, which is relatively long.	• State variables are well damped; however, the amplitude is higher, though still within an acceptable range. • This increase may amplify the effect of output disturbances. • The settling time is approximately 3 s, which is better than that of the cascaded control.

The conclusion that can be drawn from the above results is that the control strategy we developed in this article, namely the cascade control (local and global), offers the best results in terms of stability and performance compared to the one developed by N. Abu-Tabak.

VII. DISCUSSION AND CONCLUSION

This study highlights the effectiveness of a cascade control strategy for joint voltage and frequency regulation in a multi-machine power network. Combining a local H∞ controller with a global controller yields a system that is stable, robust, and performant under uncertainties and disturbances.

MATLAB/Editor simulation results confirm the superiority of the proposed approach: the system response remains satisfactory even in the presence of a short circuit. These performances demonstrate the ability of H∞ control to maintain network robustness while ensuring effective generator coordination.

Future research perspectives include improving the weighting functions using a dedicated optimization algorithm to reduce transient oscillations, enhance steady-state stability, and extend the method to larger-scale networks integrating renewable energy sources. Another important direction is the experimental implementation on a real-time test bench to validate the simulation results.

REFERENCES

[1]. Gupta S., Chattopadhyay S. & Parida S, " Transient stability enhancement of multimachine power system using robust pole-shifting controller for CSC-STATCOM.", International Scholarly Research Notices, 2015

[2]. N. Abu-Tabak, J. Y. Auloge & P. Auriol, « Dynamic Stability and Optimal Control of a Multi-machine Power Networks Modeling and Simulation », Presented at the International Conference on Power Systems Transients (IPST'07) in Lyon, France on June 4-7 2007.

[3]. Nesmat Abu-Tabak, « Stabilité dynamique des systèmes électriques multimachines: modélisation, commande, observation et simulation » Doctoral Thesis, Ecole Centrale de Lion, (November 19, 2008).

[4]. Y anhong Liu, Jianyong Li, Chunwen Li & Lijun Zhang, « H∞ Excitation Control of Multi-machine Multi-load Power Systems via Hamiltonian Function Method », 2010 8th IEEE International Conference on Control and Automation Xiamen, China, June 9-11, 2010.

[5]. Khodabakhshian A & Hemmati R, « Robust decentralized multi-machine power system stabilizer design using quantitative feedback theory. », International Journal of Electrical Power & Energy Systems, 41(1), 112 – 119, 2012.

[6]. Fathollahi A & Andresen B, « Multi-Machine Power System Transient Stability Enhancement Utilizing a Fractional Order-Based Nonlinear Stabilizer. », Fractal and Fractional, 7(11), 808, 2023.

[7]. Fathollahi A, Andresen B, « Enhancing Transient Stability in Multi-Machine Power Systems through a Model-Free Fractional-Order Excitation Stabilizer.», Fractal and Fractional, 8(7), 419, 2024.

[8]. P. KUNDUR, « Power system stability and control » Electric Power Research Institute, 1994.

[9]. KUNDUR .P & al, « Definition and classification of power system stability »,

IEEE Transactions on Power Systems. », 19(2), 1387 – 1401.

[10]. Andersoson .P .M & Fouad .A .A, « Power System Control and Stability (2nd ed) », IEEE Press / Wiley, 2003.

[11]. Machowski .J, Bialek .J & Bumby .J, « Power system dynamics : Stability and control (2nd ed) », Wiley, 2011.

[12]. Zhou .K, Doyle .J .C, & Glover .K, « Robust and Optimal Control », Prentice Hall, 1996.

[13]. Gilles Duc & Stéphane Font, « Commande H_∞ et μ-analyse : des outils pour la robustesse », HERMES Science Publications, Paris, 1999.